

A Tensor Product Space for Studying the Interaction of Bipartite States of Light with Nanostructures

Lukas Freter^{†1}, Benedikt Zerulla², Marjan Krstić³, Christof Holzer³,
Carsten Rockstuhl^{2,3}, and Ivan Fernandez-Corbaton^{*2}

¹*Department of Applied Physics, Aalto University School of Science, FI-00076 Aalto, Finland*

²*Institute of Nanotechnology, Karlsruhe Institute of Technology (KIT), 76131 Karlsruhe, Germany*

³*Institute of Theoretical Solid State Physics, Karlsruhe Institute of Technology (KIT), 76131 Karlsruhe, Germany*

Pairs of entangled photons are important for applications in quantum nanophotonics, where their theoretical description must accommodate their bipartite character. Such character is shared at the other end of the intensity range by, for example, the two degenerate instances of the pump field involved in second-harmonic generation. Describing the interaction of nanophotonic structures with bipartite states of light is, regardless of their intensity, a challenge with important technological applications. Here, we develop a theoretical framework for studying the interaction of material structures with bipartite states of light. The basic element is the symmetrized tensor product space of two copies of an electromagnetic Hilbert space. One of the benefits inherited from the single Hilbert space is that consequences of material symmetries are readily deduced. We derive selection rules for second-order non-linear processes in objects with rotational and/or mirror symmetries. We numerically verify several selection rules by combining quantum-chemical calculations with a Maxwell solver to simulate second-harmonic generation in two different MoS₂ clusters. The computationally convenient scattering matrix method is also extended to the tensor product space when the response of the object to one part of the state is independent of the other. For such a case, we obtain the relation between the scattering matrix in the single Hilbert space and the scattering matrix for bipartite states. Such a separable case is relevant for the entanglement evolution of biphoton states interacting with nanostructures. We discuss some possibilities for accommodating the computations of non-linear effects in the framework, for example, through a non-separable scattering operator, where the response of the object to one part of the state depends on the other part.

[†]lukas.freter@aalto.fi,

*ivan.fernandez-corbaton@kit.edu

I. INTRODUCTION

Within the increasing interest in quantum technologies, one of the objectives of quantum nanophotonics is to exploit the quantum properties of light for applications such as spectroscopy, communication, and sensing [1–4]. Nanophotonic structures can be used to generate quantum states of light, to process and modify them, and ultimately to measure them [5–7]. These endeavors raise challenging theoretical questions such as, for example, understanding when and why the entanglement of a biphoton state survives the interaction with a nanostructure [8–10]. However, it is not just at the quantum-level where photons appear in pairs. Considering electromagnetic fields in pairs is also needed in theoretical descriptions of non-linear optical processes, such as sum-frequency generation (SFG) or spontaneous parametric down-conversion (SPDC) [11, 12]. The efficiency of these nonlinear processes can be enhanced by nanophotonic structures, such as metasurfaces made from a periodic arrangement of suitably structured individual unit cells [13–20].

The intensity of typical entangled photon sources is so low that the quantum regime is reached, where the name biphoton state is fully appropriate. Such a name is, however, not really suitable to refer to the state of the pump for second-harmonic generation. Even though two copies of the pump field are simultaneously involved in the non-linear effect inside the matter, they are both

of high intensity. We will use the term bipartite state of light, or bipartite field, to refer to the general case including both intensity limits, and reserve the term biphoton state for the quantum regime.

When dealing with bipartite states in nanophotonics, the theoretical models must describe their interaction with matter without recourse to typical simplifying approximations such as paraxial light or dipolar objects, which are often grossly violated by strongly focused fields and the electromagnetic sizes of the objects in question. In one approach, symmetries and group theory techniques are being successfully applied to both entanglement evolution and non-linear responses [8–10, 13, 14].

For classical fields and single-photon states, symmetries are very conveniently treated in an algebraic approach to light-matter interaction, where the electromagnetic fields belong to a Hilbert space, and a linear operator models the action of a given object on the fields called the scattering operator of the object. The effects of symmetries can then be treated straightforwardly. In particular, symmetry-induced selection rules forbidding specific processes can be derived with just the knowledge of the symmetries of the object, that is, without having the scattering operator at hand. Another advantage of such a setting is that the scalar product of the Hilbert space allows one to readily compute fundamental properties of the field, such as energy and momentum, as well as the transfer of such properties to the object upon light-matter interaction. The Hilbert space approach matches very well with a convenient computational tool, the T-matrix. The T-matrix is a popular and powerful approach to the computation of light-matter interactions for classical fields [21–23], which also applies to single photon

states. The T-matrix encodes the full electromagnetic response of a given object upon arbitrary illuminations. The T-matrix and the scattering operator determine each other bijectively, providing the natural computational implementation of the algebraic approach. Besides describing the response of macroscopic objects characterized by their geometry and material parameters, the T-matrix approach can also be applied to molecules [24]. One of the strengths of the T-matrix approach is that computing the T-matrix of a composite object from the T-matrices of its components is efficient, and extremely efficient in the case of periodic arrangements [25], such as metamaterials or metasurfaces. T-matrices can be obtained by Maxwell simulations in the case of macroscopic objects, and time-dependent density functional theory (TD-DFT) in the case of molecules. There are many publicly available T-matrix codes [26]. The T-matrix formalism has recently been promoted from its typical monochromatic regime to an inherently polychromatic framework [27], which allows one to systematically treat light pulses interacting with material objects. The polychromatic T-matrix setting features basis vectors and wavefunctions with well-defined and relatively simple transformation properties under the Poincaré group. Additionally, the invariant properties of the electromagnetic scalar product [28] allow one to consistently define projective measurements in the algebraic setting [29, Sec. III].

In this article, motivated by the potential benefits of the algebraic approach, we set the basis for the algebraic treatment of the interaction of bipartite states of light with material objects. As an application of the basic formalism, we derive selection rules for non-linear processes, which we verify numerically. We also investigate the extension of the T-matrix to the tensor product space. The rest of the article is organized as follows. Section II summarizes the most relevant aspects of the electromagnetic Hilbert space \mathbb{M} . In Sec. III, we extend such formalism to bipartite states, whose Hilbert space is the tensor product space $\mathbb{M}_2 = \mathbb{M} \otimes \mathbb{M}$ restricted by the bosonic permutation rule. In particular, we explain how symmetry operators and symmetry generators act in \mathbb{M}_2 , extend the scalar product from \mathbb{M} to \mathbb{M}_2 , and derive the condition of entanglement in the bipartite wavefunction. The bipartite wavefunction can encode all the possible biphoton quantum correlations in space, time, and polarization. Section IV is devoted to light-matter interactions in \mathbb{M}_2 . We introduce a vacuum state that allows us to promote states in \mathbb{M} to states in \mathbb{M}_2 . This step is crucial for treating non-linear processes such as SFG or SPDC [30, 31], where single and bipartite states are involved. The formalism built up to this point allows us to easily derive symmetry-induced selection rules for the interaction of bipartite states with material objects. As examples, we obtain selection rules for the aforementioned non-linear processes for objects that feature rotational symmetries and/or mirror symmetries. For example, we show that, for objects with discrete rotational symmetry upon a $2\pi/n$ rotation that are illuminated along the symmetry axis with circular polarizations, only the trivial $n = 1$ case and $n = 3$ case allow SFG in the forward or backward directions, and that, for the $n = 3$ case, the

two incident fields need to have the same circular polarization, since otherwise SFG is forbidden by symmetry. We also show that when a mirror symmetric object is illuminated with bipartite fields whose individual linear polarizations are eigenstates of the mirror reflection, the output polarization on any scattering direction contained in the symmetry plane is fixed: transverse magnetic (TM) if the two incident fields have the same linear polarization (TE–TE or TM–TM), and transverse electric (TE) if they have different polarizations (TE–TM). Section V contains simulation results that confirm all the tested cases of the selection rules. The simulations of the second-harmonic generation in two different MoS₂ clusters are made possible by the combination of (TD-DFT) with a solver of Maxwell equations using the Hyper-T-matrix approach [32]. In Sec. VI, we investigate the extension of the T-matrix to \mathbb{M}_2 . We derive the T-matrix for bipartite states when the response of the object is separable, that is, when the response to one part of the state *does not* depend on the other part. In this case, T_2 , the T-matrix in \mathbb{M}_2 , can be obtained from the T-matrix in \mathbb{M} straightforwardly. The result differs from some expressions in the literature. We then discuss how the treatment of non-linear processes requires further research because the separability assumption no longer holds. For example, in SFG, one part of the bipartite state influences the response of the material object to the other part, which indicates the need for non-separable operators.

We highlight two benefits that the setting in \mathbb{M}_2 also inherits from the setting in \mathbb{M} [27]: i) the ability to treat general polychromatic fields, such as short light pulses, and ii) the well-defined transformations of states of light upon Lorentz boosts [33], which can be useful in the context of satellite quantum communications.

We expect that the algebraic formalism will become a useful tool for studying and engineering the interaction of bipartite states of light with nanostructures and arrangements thereof.

It is interesting to note that the extension of theories from a Hilbert space onto the tensor product of two copies of such Hilbert space, which is often known as “double copy”, has been used in formulations of gravity, analogies between light and gravitation, in particular mapping bipartite states of light to gravitational waves, and in the study of bipartite entanglement, for example [34–38].

II. SINGLE PHOTON STATES

We start by briefly reviewing the theoretical framework for single photon states and classical fields. For a more detailed overview, see [27, 39, 40]. Let \mathbb{M} denote the Hilbert space containing all free field solutions to Maxwell’s equations. Then every state $|\phi\rangle \in \mathbb{M}$ satisfying the normalization condition $\langle\phi|\phi\rangle = 1$ can be identified as a *single photon state* [28, 41, 42]. One of the reasons why \mathbb{M} is suitable to treat both classical fields and single photons is that when $\langle\phi|\phi\rangle = 1$, the electromagnetic fields describe a single photon, and when $\langle\phi|\phi\rangle \gg 1$, they describe a classical field. Similarly, the extension to bipartite states will be suitable for describing bipartite beams

of very different intensities, such as the very low fluence sources of entangled photons or the two copies of the laser field involved in second-harmonic generation (SHG).

It is convenient to express arbitrary states in \mathbb{M} as the superposition of a chosen set of basis states, where common basis states are plane waves or spherical waves. The latter are also known as vectors spherical harmonics, or multipolar fields. Within this article, we use the plane wave expansion

$$|\phi\rangle = \sum_{\lambda=\pm 1} \int_{\mathbb{R}^3 \setminus \{0\}} \frac{d^3 \mathbf{k}}{|\mathbf{k}|} \phi_\lambda(\mathbf{k}) |\mathbf{k} \lambda\rangle, \quad (1)$$

where $|\mathbf{k} \lambda\rangle$ is a plane wave state with wave vector \mathbf{k} and helicity $\lambda = \pm 1$ (polarization handedness) defined as

$$|\mathbf{k} \lambda\rangle = \sqrt{\frac{c\hbar}{\epsilon_0}} \frac{1}{\sqrt{2}} \frac{1}{\sqrt{(2\pi)^3}} |\mathbf{k}| \hat{e}_\lambda(\hat{\mathbf{k}}) \exp(-i\omega t) \exp(i\mathbf{k} \cdot \mathbf{r}). \quad (2)$$

Here, c is the speed of light in vacuum, \hbar is the reduced Planck constant, ϵ_0 the vacuum permittivity, $\omega = c|\mathbf{k}|$, and $\hat{e}_\lambda(\hat{\mathbf{k}})$ is the unit polarization handedness vector with $\hat{\mathbf{k}} = \mathbf{k}/|\mathbf{k}|$. Note that the plane wave defined in Eq. (2) is proportional to the absolute value of the wave vector, which ensures that the plane wave transforms unitarily under Lorentz boosts [27]. From now on, we will drop the summation and integration bounds in the plane wave expansion and it is understood, that we always sum over both helicities ± 1 and integrate over \mathbb{R}^3 excluding the origin. The scalar product in \mathbb{M} can then be written as:

$$\langle \phi | \psi \rangle = \sum_\lambda \int \frac{d^3 \mathbf{k}}{|\mathbf{k}|} \phi_\lambda^*(\mathbf{k}) \psi_\lambda(\mathbf{k}). \quad (3)$$

The complex expansion coefficient function, or the wave function, is given by the scalar product $\langle \mathbf{k} \lambda | \phi \rangle = \phi_\lambda(\mathbf{k})$, which requires the orthogonality relation between plane waves

$$\langle \mathbf{k} \lambda | \bar{\mathbf{k}} \bar{\lambda} \rangle = \delta_{\lambda\bar{\lambda}} \delta(\mathbf{k} - \bar{\mathbf{k}}) |\mathbf{k}|. \quad (4)$$

In this algebraic setting, transformations such as space-time translations or rotations are unitary linear operators that map states in \mathbb{M} back to \mathbb{M} . The scattering of light off an object is described by a linear scattering operator S , that acts on an incoming state to produce a corresponding outgoing state

$$|\phi_{\text{out}}\rangle = S |\phi_{\text{in}}\rangle. \quad (5)$$

To arrive at the representation of Eq. (5) in the plane wave basis, we expand the input and output state in plane waves according to Eq. (1)

$$\sum_{\bar{\lambda}} \int \frac{d^3 \bar{\mathbf{k}}}{|\bar{\mathbf{k}}|} \phi_{\text{out},\bar{\lambda}}(\bar{\mathbf{k}}) |\bar{\mathbf{k}} \bar{\lambda}\rangle = S \sum_{\lambda} \int \frac{d^3 \bar{\mathbf{k}}}{|\bar{\mathbf{k}}|} \phi_{\text{in},\lambda}(\bar{\mathbf{k}}) |\bar{\mathbf{k}} \bar{\lambda}\rangle. \quad (6)$$

After projecting onto the $|\mathbf{k} \lambda\rangle$ plane wave and making use of the orthogonality of plane waves, we arrive at the intuitive relation

$$\phi_{\text{out},\lambda}(\mathbf{k}) = \sum_{\bar{\lambda}} \int \frac{d^3 \bar{\mathbf{k}}}{|\bar{\mathbf{k}}|} \phi_{\text{in},\bar{\lambda}}(\bar{\mathbf{k}}) S_{\lambda\bar{\lambda}}(\mathbf{k}, \bar{\mathbf{k}}), \quad (7)$$

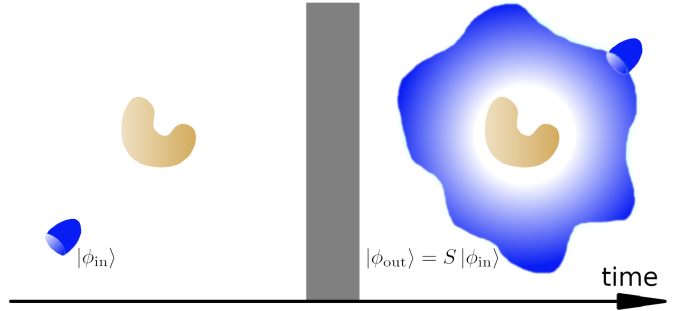


FIG. 1. Depiction of a typical scattering scenario. Before the light-matter interaction (left), an arbitrary field $|\phi_{\text{in}}\rangle \in \mathbb{M}$ is incident on an object described by the scattering operator S . \mathbb{M} is the Hilbert space of free solutions of Maxwell equations. After a finite interaction time (gray area), the scattered field is again a member of \mathbb{M} because we assume that all interactions with the object have subsided. The scattered field (right) is therefore given by $|\phi_{\text{out}}\rangle = S |\phi_{\text{in}}\rangle$.

where $S_{\lambda\bar{\lambda}}(\mathbf{k}, \bar{\mathbf{k}}) = \langle \mathbf{k} \lambda | S | \bar{\mathbf{k}} \bar{\lambda} \rangle$ is the plane wave representation of the scattering operator.

A sketch of a scattering scenario is depicted in Fig. 1. On the left, before the scattering process, the field $|\phi_{\text{in}}\rangle \in \mathbb{M}$ propagates towards the scattering object. During the light-matter interaction (gray area in Fig. 1), complicated processes can occur and, in general, the fields are not members of \mathbb{M} anymore. However, after all interactions with the object have subsided, the outgoing field propagates in free space and is again a member of \mathbb{M} . This is the justification of Eq. (5).

If the operator X describes a symmetry of the scatterer, e.g., rotation or translation, then the scattering operator commutes with the symmetry operator:

$$[S, X] = 0 \iff SX = XS \iff S = XSX^{-1}, \quad (8)$$

where the inverse exists because X represents a symmetry transformation and must hence be unitary. This simple relation can be used to derive general selection rules, see [43] for a specific application.

We note that this formalism applies to general polychromatic solutions of Maxwell's equations, such as short laser pulses, for instance.

In some cases, bases other than plane waves are more convenient, such as the basis of multipolar fields. Then, a change of basis allows one to obtain the multipolar basis vectors readily, the multipolar wave function, and the corresponding expression of the scalar product [27], with which the extension to bipartite states can be carried out following steps parallel to those that we will now take using the plane wave basis.

III. BIPARTITE STATES AND THEIR PROPERTIES

The formalism introduced in Sec. II is unsuitable to describe light-matter interaction processes where the quantum properties of multiple photons are involved, for

example, the interaction of entangled biphoton states with nanostructures. Moreover, the formalism does not cover non-linear processes, such as, for example, second-harmonic generation (SHG): The interaction of two incoming fields of the same frequency in matter creates one field with twice the energy. The process is called sum-frequency generation (SFG) when the two input fields have different frequencies. The inverse of such processes is called spontaneous parametric down-conversion (SPDC), where a single field interacts with matter and produces two outgoing fields in an energy-conserving fashion.

The natural construction for bipartite states is built from the tensor product space $\mathbb{M}_2 = \mathbb{M} \otimes \mathbb{M}$ restricted by the bosonic permutation symmetry. In the remainder of this section, we will establish the basic properties of bipartite states.

A bipartite plane wave state is expressed as

$$|\mathbf{k}\lambda, \bar{\mathbf{k}}\bar{\lambda}\rangle_2 = \frac{1}{\sqrt{2}}(|\mathbf{k}\lambda\rangle \otimes |\bar{\mathbf{k}}\bar{\lambda}\rangle + |\bar{\mathbf{k}}\bar{\lambda}\rangle \otimes |\mathbf{k}\lambda\rangle) \quad (9)$$

if $|\mathbf{k}\lambda\rangle \neq |\bar{\mathbf{k}}\bar{\lambda}\rangle$ and otherwise as

$$|\mathbf{k}\lambda, \mathbf{k}\lambda\rangle_2 = |\mathbf{k}\lambda\rangle \otimes |\mathbf{k}\lambda\rangle. \quad (10)$$

Here, the subscript 2 indicates that the ket is a member of \mathbb{M}_2 , and the bosonic permutation symmetry is satisfied due to the plus sign in Eq. (9). A minus sign would satisfy the fermionic case. Therefore, not all possible tensor products of states in \mathbb{M} are valid bipartite states. Such a definition follows the usual convention of symmetrized many-particle states, see, e.g., [44, Sec. 2.1]. For the sake of readability, the tensor product sign " \otimes " will often be dropped from now on, as in $|\mathbf{k}\lambda\rangle \otimes |\bar{\mathbf{k}}\bar{\lambda}\rangle \equiv |\mathbf{k}\lambda\rangle |\bar{\mathbf{k}}\bar{\lambda}\rangle$. It is worth emphasizing that $|\mathbf{k}\lambda, \bar{\mathbf{k}}\bar{\lambda}\rangle_2$ is not the same as $|\mathbf{k}\lambda\rangle |\bar{\mathbf{k}}\bar{\lambda}\rangle$ in general, but only if both single-photon plane waves are identical. One can expand any bipartite state as a superposition of plane waves

$$|\phi\rangle_2 = \sum_{\lambda\bar{\lambda}} \int \frac{d^3\mathbf{k}}{|\mathbf{k}|} \frac{d^3\bar{\mathbf{k}}}{|\bar{\mathbf{k}}|} \phi_{\lambda\bar{\lambda}}(\mathbf{k}, \bar{\mathbf{k}}) |\mathbf{k}\lambda, \bar{\mathbf{k}}\bar{\lambda}\rangle_2, \quad (11)$$

where $\phi_{\lambda\bar{\lambda}}(\mathbf{k}, \bar{\mathbf{k}})$ is any normalizable (wave) function with respect to the scalar product in Eq. (15). Note that there is a redundancy in the expansion in Eq. (11) in the case of $|\mathbf{k}\lambda\rangle \neq |\bar{\mathbf{k}}\bar{\lambda}\rangle$. Due to the permutation symmetry of the bipartite plane wave states $|\mathbf{k}\lambda, \bar{\mathbf{k}}\bar{\lambda}\rangle_2 = |\bar{\mathbf{k}}\bar{\lambda}, \mathbf{k}\lambda\rangle_2$, both $\phi_{\lambda\bar{\lambda}}(\mathbf{k}, \bar{\mathbf{k}})$ and $\phi_{\bar{\lambda}\lambda}(\bar{\mathbf{k}}, \mathbf{k})$ contribute to the same state. We may therefore define the symmetrized wave function

$$\Phi_{\lambda\bar{\lambda}}(\mathbf{k}, \bar{\mathbf{k}}) = \Phi_{\bar{\lambda}\lambda}(\bar{\mathbf{k}}, \mathbf{k}) = \frac{1}{\sqrt{2}} [\phi_{\lambda\bar{\lambda}}(\mathbf{k}, \bar{\mathbf{k}}) + \phi_{\bar{\lambda}\lambda}(\bar{\mathbf{k}}, \mathbf{k})], \quad (12)$$

with which the expansion in Eq. (11) is expressed as

$$|\phi\rangle_2 = \sum_{\lambda\bar{\lambda}} \int \frac{d^3\mathbf{k}}{|\mathbf{k}|} \frac{d^3\bar{\mathbf{k}}}{|\bar{\mathbf{k}}|} \Phi_{\lambda\bar{\lambda}}(\mathbf{k}, \bar{\mathbf{k}}) |\mathbf{k}\lambda\rangle |\bar{\mathbf{k}}\bar{\lambda}\rangle. \quad (13)$$

From Eq. (13), the wave function is given by $\Phi_{\lambda\bar{\lambda}}(\mathbf{k}, \bar{\mathbf{k}}) = (\langle \mathbf{k}\lambda | \bar{\mathbf{k}}\bar{\lambda} \rangle | \phi \rangle_2)$. If both parts in the bipartite state are identical, the wave function $\phi_{\lambda\lambda}(\mathbf{k}, \mathbf{k})$ is already

symmetrized, and in analogy to Eq. (12), it follows $\Phi_{\lambda\lambda}(\mathbf{k}, \mathbf{k}) = \phi_{\lambda\lambda}(\mathbf{k}, \mathbf{k})$. This relation becomes also clear when comparing the plane wave expansion in Eq. (11) to Eq. (13) in the case of identical plane waves in \mathbb{M} .

The form of Eq. (13) is reminiscent of other expansions of bipartite states, such as [30, Eq. (15)] for SPDC states. However, Eq. (13) can encode the most general quantum correlations in space, time, and polarization. Moreover, it inherits simple transformation properties in the Poincaré group from the wavefunction in \mathbb{M} [27]. Such simplicity should be advantageous for studying the effects of Lorentz boosts in general bipartite states.

The scalar product between two states in the product space \mathbb{M}_2 can be defined using the scalar product in the original space \mathbb{M} . Specifically, the natural definition is

$$(\langle \phi_1 | \langle \phi_2 |) (| \psi_1 \rangle | \psi_2 \rangle) = \langle \phi_1 | \psi_1 \rangle \langle \phi_2 | \psi_2 \rangle, \quad (14)$$

where $|\phi_{1,2}\rangle, |\psi_{1,2}\rangle \in \mathbb{M}$. For two generic bipartite states $|\phi\rangle_2$ and $|\psi\rangle_2$, the scalar product can be straightforwardly written in the plane wave basis using Eq. (13) and the orthogonality relation between plane waves in \mathbb{M} Eq. (4):

$${}_2\langle \psi | \phi \rangle_2 = \sum_{\lambda\bar{\lambda}} \int \frac{d^3\mathbf{k}}{|\mathbf{k}|} \frac{d^3\bar{\mathbf{k}}}{|\bar{\mathbf{k}}|} \Psi_{\lambda\bar{\lambda}}^*(\mathbf{k}, \bar{\mathbf{k}}) \Phi_{\lambda\bar{\lambda}}(\mathbf{k}, \bar{\mathbf{k}}). \quad (15)$$

Inspecting Eq. (3), it is clear that Eq. (15) is a natural extension of the scalar product for bipartite states.

We anticipate that the scalar product in \mathbb{M}_2 can be used to define projective measurements in \mathbb{M}_2 consistently. One of the most important properties of the scalar product in \mathbb{M} is its invariance under the transformations of the conformal group [28], which includes the Poincaré group. This implies that, for any pair $|\psi\rangle, |\phi\rangle$ in \mathbb{M} , and X in the conformal group, it holds that $\langle \psi | \phi \rangle = \langle \psi | X^\dagger X | \phi \rangle$. That is, the scalar product is invariant when the states are transformed with a conformal transformation: $|\psi\rangle \rightarrow X |\psi\rangle$, and $|\phi\rangle \rightarrow X |\phi\rangle$. Since the conformal group in Minkowski space is the largest group of invariance of Maxwell equations [45], the invariance property allows one to define projective measurements by a generic detector mode $|d\rangle$, as $|\langle d | \phi \rangle|^2$, and be assured that their value is the same in all the allowed changes of reference frame [29, Sec. III]. The structure of Eq. (15) strongly indicates that a very similar definition should be possible in \mathbb{M}_2 .

A. Separable and entangled bipartite states

A general bipartite state is said to be separable, and hence *not entangled*, if it can be factorized into two independent states in \mathbb{M}

$$|\phi\rangle_2 = \frac{1}{\sqrt{2}} (|\psi\rangle |\varphi\rangle + |\varphi\rangle |\psi\rangle), \quad |\psi\rangle, |\varphi\rangle \in \mathbb{M}. \quad (16)$$

We can substitute general states in \mathbb{M} from Eq. (1) for $|\psi\rangle$ and $|\varphi\rangle$ into Eq. (16):

$$|\phi\rangle_2 = \frac{1}{\sqrt{2}} \sum_{\lambda} \int \frac{d^3\mathbf{k}}{|\mathbf{k}|} \psi_{\lambda}(\mathbf{k}) |\mathbf{k}\lambda\rangle \otimes \sum_{\bar{\lambda}} \int \frac{d^3\bar{\mathbf{k}}}{|\bar{\mathbf{k}}|} \varphi_{\bar{\lambda}}(\bar{\mathbf{k}}) |\bar{\mathbf{k}}\bar{\lambda}\rangle + \frac{1}{\sqrt{2}} \sum_{\bar{\lambda}} \int \frac{d^3\bar{\mathbf{k}}}{|\bar{\mathbf{k}}|} \varphi_{\bar{\lambda}}(\bar{\mathbf{k}}) |\bar{\mathbf{k}}\bar{\lambda}\rangle \otimes \sum_{\lambda} \int \frac{d^3\mathbf{k}}{|\mathbf{k}|} \psi_{\lambda}(\mathbf{k}) |\mathbf{k}\lambda\rangle, \quad (17)$$

which is easily brought into the following form

$$|\phi\rangle_2 = \frac{1}{\sqrt{2}} \sum_{\lambda\bar{\lambda}} \int \frac{d^3\mathbf{k}}{|\mathbf{k}|} \frac{d^3\bar{\mathbf{k}}}{|\bar{\mathbf{k}}|} \psi_{\lambda}(\mathbf{k}) \varphi_{\bar{\lambda}}(\bar{\mathbf{k}}) \times (|\mathbf{k}\lambda\rangle |\bar{\mathbf{k}}\bar{\lambda}\rangle + |\bar{\mathbf{k}}\bar{\lambda}\rangle |\mathbf{k}\lambda\rangle) = \sum_{\lambda\bar{\lambda}} \int \frac{d^3\mathbf{k}}{|\mathbf{k}|} \frac{d^3\bar{\mathbf{k}}}{|\bar{\mathbf{k}}|} \psi_{\lambda}(\mathbf{k}) \varphi_{\bar{\lambda}}(\bar{\mathbf{k}}) |\mathbf{k}\lambda, \bar{\mathbf{k}}\bar{\lambda}\rangle_2. \quad (18)$$

Comparing Eq. (18) with Eq. (11), we find the foreseeable separability condition for the bipartite wave function

$$\phi_{\lambda\bar{\lambda}}(\mathbf{k}, \bar{\mathbf{k}}) = \psi_{\lambda}(\mathbf{k}) \varphi_{\bar{\lambda}}(\bar{\mathbf{k}}). \quad (19)$$

In general, the $\phi_{\lambda\bar{\lambda}}(\mathbf{k}, \bar{\mathbf{k}})$ in Eq. (11) does not necessarily meet Eq. (19), in which case the bipartite state is entangled.

B. Symmetry transformations

Symmetry transformations play an essential role in the algebraic description of electromagnetics because they are intimately linked to conservation laws, that is, the Noether theorem. The action of common symmetry transformations, such as space-time translation, rotations, duality, parity, and mirror symmetries, on bipartite states, can be inferred from their well-known action on states in \mathbb{M} .

Let X be an arbitrary symmetry transformation acting on states in \mathbb{M} . The action of the same transformation on a bipartite state in \mathbb{M}_2 is then given by [46, Sec. 3.8]:

$$X_2 = X \otimes X. \quad (20)$$

As an example, if X describes the spatial translation in \mathbb{M} by the displacement vector \mathbf{s} , as $X = \mathbf{T}(\mathbf{s})$, we know that

$$\mathbf{T}(\mathbf{s}) |\mathbf{k}\lambda\rangle = \exp(-i\mathbf{k} \cdot \mathbf{s}) |\mathbf{k}\lambda\rangle. \quad (21)$$

Translating a bipartite plane wave state by \mathbf{s} is thus achieved by

$$\begin{aligned} \mathbf{T}_2(\mathbf{s}) |\mathbf{k}\lambda, \bar{\mathbf{k}}\bar{\lambda}\rangle_2 &= \frac{1}{\sqrt{2}} (\mathbf{T}(\mathbf{s}) |\mathbf{k}\lambda\rangle \otimes \mathbf{T}(\mathbf{s}) |\bar{\mathbf{k}}\bar{\lambda}\rangle + \mathbf{T}(\mathbf{s}) |\bar{\mathbf{k}}\bar{\lambda}\rangle \otimes \mathbf{T}(\mathbf{s}) |\mathbf{k}\lambda\rangle) \\ &= \exp[-i(\mathbf{k} + \bar{\mathbf{k}}) \cdot \mathbf{s}] |\mathbf{k}\lambda, \bar{\mathbf{k}}\bar{\lambda}\rangle_2, \end{aligned} \quad (22)$$

showing that $|\mathbf{k}\lambda, \bar{\mathbf{k}}\bar{\lambda}\rangle_2$ is an eigenstate of translations. If the symmetry transformation X is continuous, as in the

case of spatial translations, it can be expressed by the exponential of a generator Γ , namely as $X(\theta) = \exp(-i\theta\Gamma)$. The generator of spatial translations is the momentum \mathbf{P} , resulting in $\mathbf{T}(\mathbf{s}) = \exp(-i\mathbf{P} \cdot \mathbf{s}/\hbar)$. The generator of a continuous symmetry transformation in the tensor product space \mathbb{M}_2 can be obtained from the generator in \mathbb{M} as

$$\Gamma_2 = \Gamma \otimes \mathbb{1} + \mathbb{1} \otimes \Gamma, \quad (23)$$

by considering the terms that are linear in θ in the expansion of $X_2(\theta \rightarrow 0)$ [46, Eq. (7.7-4)].

If an operator O_2 in \mathbb{M}_2 commutes with a continuous symmetry $X_2(\theta) = \exp(-i\theta\Gamma_2)$, then it also commutes with its generator, and the converse statement is also true:

$$O_2 X_2(\theta) = X_2(\theta) O_2 \iff O_2 \Gamma_2 = \Gamma_2 O_2. \quad (24)$$

The above statement holds for operators in \mathbb{M} as well.

Notably, we highlight that the transformation properties of bipartite states under Lorentz boosts can be readily obtained using Eq. (20) with X representing a Lorentz boost, and the transformation properties of $|\mathbf{k}\lambda\rangle$ under such transformations [27].

IV. LIGHT-MATTER INTERACTION IN \mathbb{M}_2

A. General setting and emergence of non-linearity

In a scattering scenario in \mathbb{M}_2 , we are interested in the fields $|\phi_{\text{out}}\rangle_2$ after the interaction of some incoming field $|\phi_{\text{in}}\rangle_2$ with a scattering object, analogous to Fig. 1 in \mathbb{M} . Again, we assume that both incoming and outgoing fields are members of \mathbb{M}_2 , which is valid as long as the incoming field is considered before it enters into contact with the object, and the outgoing field is considered after all the interactions with the scatterer have subsided. In that case, the scattering scenario boils down to a *linear transformation* in \mathbb{M}_2 , which maps the incoming field to the outgoing field $S_2 : \mathbb{M}_2 \rightarrow \mathbb{M}_2$. In analogy to Eq. (5) for states in \mathbb{M} , we have

$$|\phi_{\text{out}}\rangle_2 = S_2 |\phi_{\text{in}}\rangle_2 \quad (25)$$

for bipartite states. Now, one of the motivations for studying bipartite scattering is the description of non-linear processes with the Hilbert space approach. However, Eq. (25) shows a linear relation between incoming and outgoing states. To see how the non-linearity comes about, let us expand incoming and outgoing fields and the scattering operator in the plane wave basis. After some simple algebra, we arrive at the following equation relating the wave function of the incoming field to the wave function of the outgoing field

$$\Phi_{\lambda\bar{\lambda}}^{\text{out}}(\mathbf{k}, \bar{\mathbf{k}}) = \sum_{\sigma\bar{\sigma}} \int \frac{d^3\mathbf{q}}{|\mathbf{q}|} \frac{d^3\bar{\mathbf{q}}}{|\bar{\mathbf{q}}|} S_{2,\lambda\bar{\lambda}\sigma\bar{\sigma}}(\mathbf{k}, \bar{\mathbf{k}}, \mathbf{q}, \bar{\mathbf{q}}) \Phi_{\sigma\bar{\sigma}}^{\text{in}}(\mathbf{q}, \bar{\mathbf{q}}) \quad (26)$$

with

$$S_{2,\lambda\bar{\lambda}\sigma\bar{\sigma}}(\mathbf{k}, \bar{\mathbf{k}}, \mathbf{q}, \bar{\mathbf{q}}) = (\langle \mathbf{k}\lambda | \langle \bar{\mathbf{k}}\bar{\lambda} |) S_2 (| \mathbf{q}\sigma \rangle | \bar{\mathbf{q}}\bar{\sigma} \rangle). \quad (27)$$

This is completely analogous to Eqs. (6) and (7) for states in \mathbb{M} . For clarity purposes, let us assume that in SHG the incoming field is a separable bipartite state with two equal fields described by the wave function $a_\lambda(\mathbf{k})$. Using Eq. (12) we find $\Phi_{\sigma\bar{\sigma}}^{\text{in}}(\mathbf{q}, \bar{\mathbf{q}}) = \sqrt{2}a_\sigma(\mathbf{q})a_{\bar{\sigma}}(\bar{\mathbf{q}})$ and note in passing that $\Phi_{\sigma\sigma}^{\text{in}}(\mathbf{q}, \mathbf{q}) = a_\sigma^2(\mathbf{q})$. By interpreting the wave function $a_\lambda(\mathbf{k})$ as the amplitude of the incoming field, Eq. (26) shows that the outgoing wave function depends on the product of two incoming fields, weighted by the appropriate scattering coefficient. Thus, the non-linearity appears with respect to the single photons or classical fields, whereas the scattering in \mathbb{M}_2 is purely linear.

The form of the scattering operator in Eq. (26) is fully general. We will show in Sec. VI for at least some bipartite processes that S can be assumed to be separable: $S_{2,\lambda\bar{\lambda}\sigma\bar{\sigma}}(\mathbf{k}, \bar{\mathbf{k}}, \mathbf{q}, \bar{\mathbf{q}}) = S_{\lambda\bar{\lambda}}(\mathbf{k}, \bar{\mathbf{k}})S_{\sigma\bar{\sigma}}(\mathbf{q}, \bar{\mathbf{q}})$.

It is readily shown that if the incoming bipartite state is separable, and additionally S_2 is also separable, then the outgoing bipartite state must be separable as well. The case of separable S_2 and entangled illumination has been studied for biphoton scattering in [8, 9]. The case of separable illumination but non-separable S_2 is discussed in Sec. VI. The physical meaning of a non-separable S_2 is that the material response to one piece of the bipartite illumination depends on the other piece.

B. The vacuum state

In non-linear optical processes such as SFG or SPDC, the number of photons changes, which in the algebraic setting can be seen as going from \mathbb{M}_2 to \mathbb{M} or vice versa. However, the scattering operator S_2 maps bipartite states onto bipartite states. For the bipartite formalism to accommodate single states in \mathbb{M} , we need to introduce the vacuum state $|0\rangle$. The vacuum state has zero photons and is defined by the following properties

$$\begin{aligned} \langle \mathbf{k} \lambda | 0 \rangle &= 0, & \langle 0 | 0 \rangle &= 1 \\ X(\theta) | 0 \rangle &= | 0 \rangle, & \Gamma | 0 \rangle &= 0, & X(\theta) &= \exp(-i\Gamma\theta). \end{aligned} \quad (28)$$

Namely, it is a normalized state that is orthogonal to every plane wave state. It is additionally invariant under any symmetry transformation $X(\theta)$. This implies that any generator Γ generating a symmetry transformation acting on the vacuum yields zero [47, Sec. 1-4]. The condition $\langle \mathbf{k} \lambda | 0 \rangle = 0$ implies by linearity that the vacuum state is orthogonal to any state in \mathbb{M} , which intuitively makes sense since the probability of finding a state in \mathbb{M} with zero photons is zero.

The scalar products in the first line of Eq. (28), involving the vacuum state, are different than the scalar product between two members of \mathbb{M} in Eq. (3). In particular, $\langle 0 | 0 \rangle$ does not imply that the vacuum contains one photon. The vacuum state can be more rigorously built in as the only member of a one-dimensional Hilbert space [44, Sec. 2.1], and the following construction in Eq. (29) can be understood as a tensor product of a plane wave in \mathbb{M} and the lone state in such one-dimensional Hilbert space. For convenience, we nevertheless use the same notation.

We now define the state

$$|\mathbf{k} \lambda, 0\rangle_2 = |\mathbf{k} \lambda\rangle |0\rangle \quad (29)$$

which we can rigorously identify with the state $|\mathbf{k} \lambda\rangle$ by checking that when the symmetry transformations of the Poincaré group act on Eq. (29), they produce exactly the same effect as on $|\mathbf{k} \lambda\rangle$. Thus, the vacuum state allows us to write any state in \mathbb{M} as a bipartite state, which includes the vacuum $|0\rangle$.

The tensor product notation that we use does not feature the creation and annihilation operators of second quantization. Since we are at most dealing with bipartite states, the notational advantage of second quantization for tensor products of many copies of \mathbb{M} is not too pronounced [44, Chap. 2]. The notation we employ comes from the algebraic setting in \mathbb{M} . One can argue that it affords a more direct treatment of symmetries and their consequences using the results from \mathbb{M} , even though they can certainly be dealt with in the framework of second quantization [8–10].

C. Selection rules for second-order non-linear processes

In this subsection, we outline several examples of selection rules upon scattering in \mathbb{M}_2 , reproducing known outcomes, and obtaining some new results. Even though the main focus will be on second-order non-linear processes, we will also comment on generalizations to third- and N th-order non-linear processes.

To start, we assume that the incoming bipartite state is a separable state of two plane waves in \mathbb{M} . We will derive the selection rules for SFG. However, the structure of the derivations makes it clear that the selection rules also apply to the inverse SPDC process.

The SFG process can be exemplified by Eq. (25) with incoming and outgoing fields given by

$$\begin{aligned} |\phi_{\text{in}}\rangle_2 &= |\mathbf{k}_1 \lambda_1, \mathbf{k}_2 \lambda_2\rangle_2, & |\phi_{\text{out}}\rangle_2 &= |\mathbf{k}_3 \lambda_3, 0\rangle_2, \\ \omega_i &= c|\mathbf{k}_i|, & i &= 1, 2, 3. \end{aligned} \quad (30)$$

In the following, we will use several symmetries of the scattering object to infer conservation laws and selection rules. To start, let us consider the time translation symmetry of the SFG process, which should lead to energy conservation. Time translation symmetry implies that the scattering operator commutes with the generator of time translations, that is, the energy operator

$$S_2 H_2 = H_2 S_2. \quad (31)$$

Let us apply the energy operator to both incoming and outgoing states in Eq. (30):

$$\begin{aligned} H_2 |\phi_{\text{in}}\rangle_2 &= (H \otimes \mathbb{1} + \mathbb{1} \otimes H) \frac{1}{\sqrt{2}} (|\mathbf{k}_1 \lambda_1\rangle |\mathbf{k}_2 \lambda_2\rangle + |\mathbf{k}_2 \lambda_2\rangle |\mathbf{k}_1 \lambda_1\rangle) \\ &= \hbar(\omega_1 + \omega_2) |\mathbf{k}_1 \lambda_1, \mathbf{k}_2 \lambda_2\rangle_2 \end{aligned} \quad (32)$$

and

$$\begin{aligned} H_2 |\phi_{\text{out}}\rangle_2 &= (H \otimes \mathbb{1} + \mathbb{1} \otimes H) |\mathbf{k}_3 \lambda_3\rangle |0\rangle \\ &= \hbar\omega_3 |\mathbf{k}_3 \lambda_3, 0\rangle_2 \end{aligned} \quad (33)$$

where the well known relation for states in \mathbb{M} , $H |\mathbf{k} \lambda\rangle = \hbar\omega |\mathbf{k} \lambda\rangle$, is used. With the symmetry relation of Eq. (31), we find another expression for the energy of the outgoing state,

$$\begin{aligned} H_2 |\phi_{\text{out}}\rangle_2 &= H_2 S_2 |\phi_{\text{in}}\rangle_2 \\ &= S_2 H_2 |\phi_{\text{in}}\rangle_2 \\ &= S_2 \hbar(\omega_1 + \omega_2) |\phi_{\text{in}}\rangle_2 \\ &= \hbar(\omega_1 + \omega_2) |\phi_{\text{out}}\rangle_2. \end{aligned} \quad (34)$$

Comparing Eq. (33) with Eq. (34) we find the expected relation $\omega_3 = \omega_1 + \omega_2$, which is the statement of energy conservation.

1. Rotational symmetric scatterers

Let us consider a discrete rotational symmetry of the scattering object along the propagation direction of the incoming illumination, which can be chosen to be the z -direction. The symmetry condition reads

$$S_2 = R_{z,2}(\theta_n) S_2 R_{z,2}^{-1}(\theta_n) \quad (35)$$

with

$$\theta_n = 2\pi/n, n \in \mathbb{N} \text{ and } R_{z,2}(\theta_n) = R_z(\theta_n) \otimes R_z(\theta_n). \quad (36)$$

Such discrete rotational symmetry is often written as C_n symmetry, as in C_1 (trivial), C_2 , C_3 , and so on.

We will focus on the SFG signal radiated along the z -directions. Then, the incoming and outgoing states read

$$|\phi_{\text{in}}\rangle_2 = |k_1 \hat{z} \lambda_1, k_2 \hat{z} \lambda_2\rangle_2, \quad |\phi_{\text{out}}\rangle_2 = |\pm k_3 \hat{z} \lambda_3, 0\rangle_2, \quad (37)$$

and the scattering amplitude for the SFG process is given by

$$A = {}_2\langle \phi_{\text{out}} | S_2 | \phi_{\text{in}} \rangle_2. \quad (38)$$

To study the implications of discrete rotational symmetry on the SFG process, we need to know how the rotation operator $R_z(\theta_n)$ acts on a state in \mathbb{M} propagating in the $\pm z$ -direction. It can be shown that [46, Sec. 9.7]

$$R_z(\theta_n) |\pm k \hat{z} \lambda\rangle = \exp(\mp i \lambda \theta_n) |\pm k \hat{z} \lambda\rangle. \quad (39)$$

To simplify the notation, from now on we will drop the unit vector \hat{z} in the plane wave states $|\pm k \hat{z} \lambda\rangle \equiv |\pm k \lambda\rangle$. It is understood that a positive (negative) sign in front of the wave number corresponds to propagation in the positive (negative) z -direction. By making use of the symmetry Eq. (35), and relation (39), we can express the scattering amplitude as

$$\begin{aligned} A &= {}_2\langle \phi_{\text{out}} | R_{z,2}(\theta_n) S_2 R_{z,2}^{-1}(\theta_n) | \phi_{\text{in}} \rangle_2 \\ &= {}_2\langle \pm k_3 \lambda_3, 0 | R_{z,2}(\theta_n) S_2 R_{z,2}^{-1}(\theta_n) | k_1 \lambda_1, k_2 \lambda_2 \rangle_2 \\ &= {}_2\langle \pm k_3 \lambda_3, 0 | S_2 \exp[i\theta_n(\lambda_1 + \lambda_2 \mp \lambda_3)] | k_1 \lambda_1, k_2 \lambda_2 \rangle_2 \\ &= \exp[i\theta_n(\lambda_1 + \lambda_2 \mp \lambda_3)] A, \end{aligned} \quad (40)$$

which tells us that unless the equality $\exp[i\theta_n(\lambda_1 + \lambda_2 \mp \lambda_3)] = 1$ holds, only the $A = 0$ solution of Eq. (40) exists. Hence, the SFG process is forbidden. For a discrete n -fold rotational symmetry, we can substitute $\theta_n = 2\pi/n$ yielding the condition

$$\exp\left[i\frac{2\pi}{n}(\lambda_1 + \lambda_2 \mp \lambda_3)\right] = 1. \quad (41)$$

Let us first consider forward SFG, implying a minus sign in Eq. (41). Three distinct cases need to be considered. First, the two incoming fields can have the same helicity, which is opposite to the helicity of the outgoing state

$$\lambda_1 = \lambda_2 = -\lambda_3 \Rightarrow \exp\left(\pm i\frac{6\pi}{n}\right) = 1. \quad (42)$$

This is only satisfied for the trivial $n = 1$ case and for the $n = 3$ case. For all other cases, SFG in the forward direction is prohibited. Second, the two parts of the incoming state and the outgoing state have the same helicity

$$\lambda_1 = \lambda_2 = \lambda_3 \Rightarrow \exp\left(\pm i\frac{2\pi}{n}\right) = 1, \quad (43)$$

resulting in zero forward SFG for all $n > 1$. Third, the two incoming fields can have different helicities, resulting in the condition

$$\lambda_1 = -\lambda_2 \Rightarrow \exp\left(i\lambda_3\frac{2\pi}{n}\right) = 1, \quad (44)$$

which is again only satisfied for $n = 1$.

We distinguish between two cases for backward SFG (plus sign in Eq. (41)). The first case is that all fields have the same helicity

$$\lambda_1 = \lambda_2 = \lambda_3 \Rightarrow \exp\left(\pm i\frac{6\pi}{n}\right) = 1 \quad (45)$$

which is again satisfied for $n = 1$ and $n = 3$. In the second case, one of the fields has a different helicity than the other two, implying that

$$\exp\left(\pm i\frac{2\pi}{n}\right) = 1 \quad (46)$$

which is again only satisfied for $n = 1$.

To summarize, except for the trivial non-symmetric case $n = 1$, the SFG process in a discrete rotationally symmetric object is only possible for $n = 3$ and only if *both incoming fields have the same helicity*. In the forward direction, the outgoing state has the opposite helicity, and in the backward direction, it has the same helicity as the incoming fields. The selection rules are illustrated in Fig. 2 and compared to the selection rules for linear scattering in \mathbb{M} [43]. Note that the selection rules rely only on the rotational symmetry of the scatterer and not on the apparent mirror symmetries suggested in this figure. So even for a chiral material, for which all mirror symmetries are broken, the selection rules hold.

In [48, 49], selection rules for SHG have been developed when both incoming fields have the same helicity,

and they agree with the selection rules derived here. Further, the experimental results in [50] are consistent with the selection rules for $n = 3$. Note, though, that in the supplementary material of the previously mentioned paper, Table S1 is partly incorrect: It indicates the possibility of SFG or SHG for objects with a six-fold rotational symmetry, which we have shown is not possible.

2. Mirror symmetric scatterers

Let us now derive selection rules for SHG for a medium with mirror symmetry across the xz -plane, which is defined by inversion across the y -axis $M_y : y \rightarrow -y$. Due to the symmetry of the system, it is convenient to switch to the TE/TM basis, defined by linear combinations of circular polarizations as $|\mathbf{k} \tau\rangle = (|\mathbf{k} +\rangle + \tau |\mathbf{k} -\rangle)/\sqrt{2}$, where $\tau = 1$ corresponds to TM polarization, and $\tau = -1$ to TE polarization. For the remainder of this section, the wave vector is assumed to be on the z -axis and is omitted as an argument of the plane wave kets. The plane wave states $|\tau\rangle$ correspond to linearly polarized states where

$$|\tau = 1\rangle \equiv |\leftrightarrow\rangle, \quad |\tau = -1\rangle \equiv |\updownarrow\rangle. \quad (47)$$

It is, therefore, easy to see that for states in \mathbb{M} , the mirror transformation acts as

$$M_y |\tau\rangle = \tau |\tau\rangle. \quad (48)$$

That is, the horizontal (TM, \hat{x}) polarization is an eigenstate of the symmetry transformation with eigenvalue $+1$, whereas the vertical (TE, \hat{y}) polarization is an eigenstate with eigenvalue -1 . Horizontal and vertical polarizations are defined with respect to the mirror plane, which is in our case the xz -plane, see Fig. 3 below representing the example that we consider to support our findings. We thus find that bipartite states with two equal polarization states are always eigenstates of the mirror symmetry with eigenvalue $+1$

$$M_{y,2} |\tau\rangle |\tau\rangle = M_y |\tau\rangle \otimes M_y |\tau\rangle = \tau^2 |\tau\rangle |\tau\rangle = |\tau\rangle |\tau\rangle. \quad (49)$$

To arrive at the selection rule for the SFG process, where two fields with polarization τ are incoming to produce one field of polarization $\bar{\tau}$, we compute the scattering amplitude

$$\begin{aligned} A &= {}_2\langle \bar{\tau}, 0 | S_2(|\tau\rangle |\tau\rangle) \\ &= {}_2\langle \bar{\tau}, 0 | M_{y,2} S_2 M_{y,2} (|\tau\rangle |\tau\rangle) \\ &= \bar{\tau} A. \end{aligned} \quad (50)$$

Equation (50) states that the SFG process is only possible for $\bar{\tau} = 1$, that is, for TM outgoing polarization, independent of the polarization of the incoming fields. Note that if the incoming fields have different linear polarization, the incoming state is an eigenstate of $M_{y,2}$ with eigenvalue -1 . Proceeding similar to (50), we find the expression $A = -\bar{\tau} A$ for the scattering amplitude, where $\bar{\tau}$ is the polarization of the outgoing photon. This

means that the SFG process is only allowed for TE outgoing polarization. The same derivation and results apply to any scattering direction on the xz -plane, for example backward reflection.

This formalism can be generalized to higher-order processes. For third-harmonic generation, for example, we find that the product of the three incoming polarizations and the outgoing polarization must be equal to one. Hence, if, for example, the three incoming polarizations are equal, then the outgoing polarizations must be the same.

3. Generalization to N th-harmonic generation

Generalizing the selection rules to an N th order non-linear process is straightforward under an n -fold discrete rotational symmetry. Therefore, we want to focus on the simplest case of N th-harmonic generation, where N fields with frequency $\omega = c|\mathbf{k}|$ and helicity λ interact to produce a single field of frequency $\bar{\omega} = N\omega = Nc|\mathbf{k}|$ and helicity $\bar{\lambda}$. Assuming propagation along the z -direction and again omitting the \hat{z} for the wave vector in the plane wave kets, the input and output states can be written as

$$|\phi_{\text{in}}\rangle_N = \underbrace{|k \lambda\rangle |k \lambda\rangle \dots |k \lambda\rangle}_{N\text{-times}} \quad (51)$$

$$|\phi_{\text{out}}\rangle_N = |\pm Nk \bar{\lambda}, 0\rangle_N \equiv |\pm Nk \bar{\lambda}\rangle \underbrace{|0\rangle |0\rangle \dots |0\rangle}_{(N-1)\text{-times}}. \quad (52)$$

The N -part states in Eq. (51) and Eq. (52) live in the tensor product space $\mathbb{M}_N = \bigotimes_{i=1}^N \mathbb{M}$ in analogy to the bipartite product space for second-order non-linear processes. Following a similar derivation as in the previous section, we arrive at the selection rules for an n -fold rotational symmetric medium

$$\exp\left[i\frac{2\pi}{n}(N\lambda \mp \bar{\lambda})\right] = 1. \quad (53)$$

In the case of forward scattering, the condition reads

$$\begin{aligned} N - 1 &= mn, \quad m \in \mathbb{Z}, \quad \text{for } \lambda = \bar{\lambda} \\ N + 1 &= mn, \quad m \in \mathbb{Z}, \quad \text{for } \lambda = -\bar{\lambda}, \end{aligned} \quad (54)$$

which is equivalent to Eq. (10) in [48]. It is possible to generalize the above selection rules by allowing e.g. the incoming fields to have different helicities. Then, we would have to make the substitution $N\lambda \rightarrow \sum_{j=1}^N \lambda_j$, where λ_j is the helicity of the j -th incoming photon.

4. Tables with the selection rules

Table I, left, shows which output polarizations for a second-order process are allowed for a given incoming polarization (in the helicity basis) when the object has a discrete rotation symmetry about the axis of incidence. In Table I, right, we list the allowed outgoing polarization of second and third-order processes for an object with M_y mirror symmetry (in TE/TM basis).

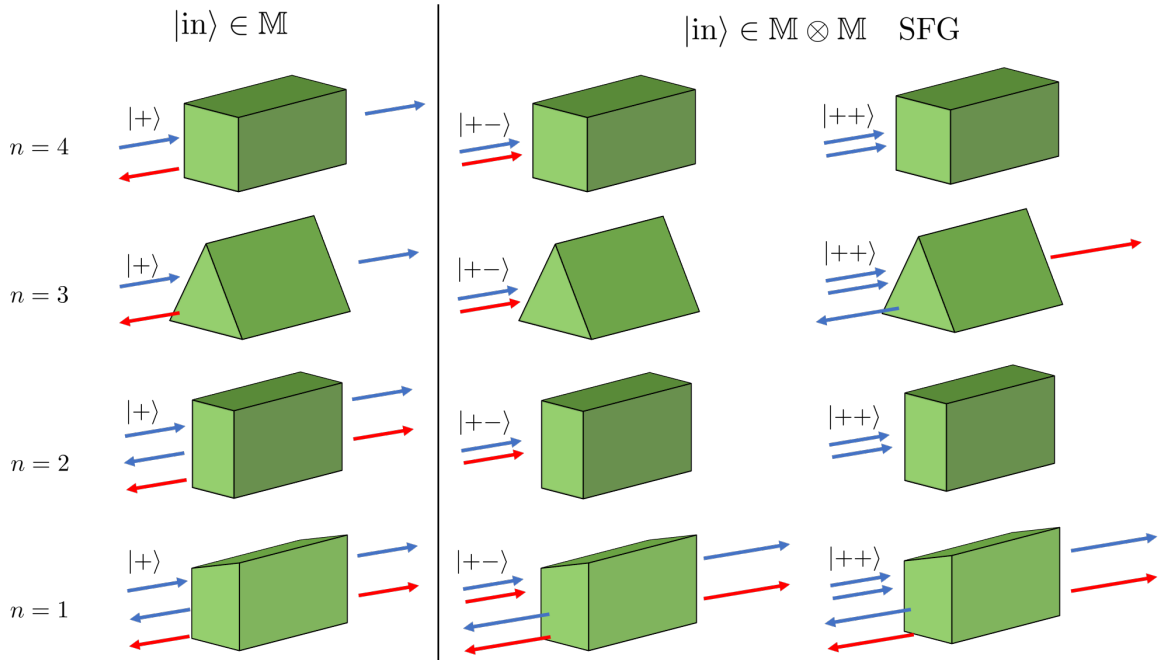


FIG. 2. Summary of the selection rules for n -fold discrete rotational symmetric scatters. Blue and red arrows indicate left and right polarization handedness, respectively. Left: Selection rules in \mathbb{M} , see Ref. [43] for details. Right: Selection rules for SFG in \mathbb{M}_2 . The cases with $n > 4$ behave as the $n = 4$ cases in both \mathbb{M} and \mathbb{M}_2 , respectively.

SFG with C_n symmetry				SFG/ THG with mirror symmetry		
n	Incident	Transm.	Ref.		Incident	Transm./ Refl.
1		+, -	+, -	SFG	TE-TE	TM
2	++	x	x		TM-TM	TM
3		-	+		TE-TM	TE
≥ 4		x	x			
1		+, -	+, -	THG	TE-TE-TE	TE
2	+-	x	x		TM-TM-TM	TM
3		x	x		TE-TE-TM	TM
≥ 3		x	x		TM-TM-TE	TE

TABLE I. Summary of allowed second- and third-order processes in transmission and reflection for an n -fold rotational symmetric object (left) and for a mirror symmetric object (right) at normal incidence. An "x" means that the process is forbidden. The allowed and forbidden processes for $--$ and $-+$ incoming polarization can be obtained by flipping all the helicities in the table.

V. SIMULATION RESULTS

In this section, we present simulation results confirming the selection rules derived above, specifically for the most interesting case of a three-fold rotation symmetry, that is, $n = 3$. We start our simulations from the molecular level by employing quantum chemical calculations based on density functional theory (DFT). Two finite-size molecular models of MoS_2 were chosen. The first one (Fig. 3 a)) has an approximately hexagonal shape, but only $R_z(2\pi/3)$ rotational symmetry, and has M_y mirror symmetry. The second molecular model (Fig. 3 b)) has a rhomboidal shape, with also M_y mirror symmetry, but does not feature any rotational symmetry along the z -axis. We applied time-dependent density functional theory (TD-DFT) calculations to calculate both the linear response, in the form of damped complex dynamic polarizability tensors including electric-electric, electric-magnetic, and magnetic-magnetic components, and the non-linear response, in the form of complex electric-

electric hyperpolarizability tensors of these two models at 800 nm and 1064 nm. The Supplementary Information VIII contains more details of the simulations. We note that we performed the calculations in a rotated coordinate system due to common point group conventions in the DFT computations. Afterward, we transferred the results to the coordinate system depicted in Fig. 3. Combining the multiple scattering software *treams* [25] with the Hyper-T-matrix formalism from [32], we can calculate the second-order non-linear response of both systems for different incoming polarizations. Specifically, for both structures shown in Fig. 3, we simulated the SHG response for normally incoming fields at the fundamental wavelength.

In the following, we discuss the simulation results for the fundamental wavelength of 800 nm. We note that the qualitative result is the same for 1064 nm. For the rhomboid structure in Fig. 3 b), the intensity of the SHG wave in transmission and reflection for TE and TM polarized incoming and outgoing fields is shown in Table II.

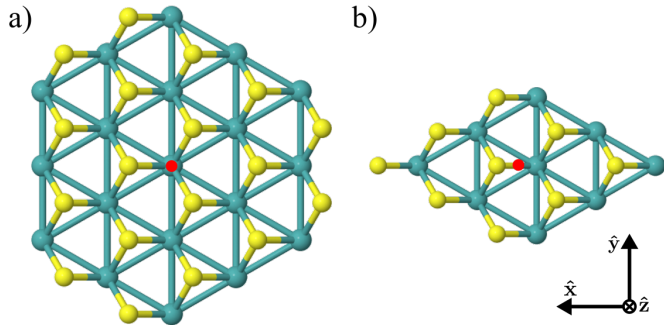


FIG. 3. The finite size molecular models of the MoS₂ clusters in **a**) with C₃ symmetry, and **b**) with rhomboidal shape and only the trivial C₁ symmetry. Both structures have the mirror symmetry $M_y : y \rightarrow -y$. In each case, the center of coordinates was placed at the red dot, which corresponds to the center of mass of the structure.

We note that we only evaluate outgoing plane waves with wave vectors on the z -axis, see Section IV C 2. We further note that all of our simulation results are normalized to the largest intensity, which occurred for two TM-polarized incoming fields in TM transmission and reflection. Then, normalized signals on the order of 10^{-5} and lower are considered numerical noise. The value 1 corresponds to an SHG conversion efficiency equal to 6.1×10^{-34} , which is very low because of the very small sizes of the clusters. As seen from the results in Table II, if the two incoming fields have the same linear polarization, then the SHG signal in transmission and reflection will only be in the TM polarization. On the contrary, if the incoming fields have different linear polarizations, only TE polarization appears in the SHG signal. This is fully consistent with the selection rules derived in Section IV C 2.

Table III shows the simulated SHG intensity for circularly polarized fields incident on the rhomboid structure. The first row shows the response where two fields at the fundamental wavelength of the same helicity, namely plus helicity, combine to give rise to a field at the second-harmonic wavelength. The results for two incoming fields with different helicities are shown in the second row. Due to the trivial C₁-symmetry, we expect SHG signals both in reflection and transmission to be present, irrespective of the polarization of the incoming helicities, as predicted in Fig. 2 for the $n = 1$ case. This is precisely what the results in Table III show, as all SHG values have the same order of magnitude.

For the other structure, which shows C₃-symmetry, the intensity of the SHG wave in transmission and reflection for both plus and minus helicity is shown in Table IV. In the case of equal incoming helicities, the intensity of the second-harmonic signal in transmission (reflection) practically vanishes if the outgoing helicity is the same (opposite) as the incoming helicity. Furthermore, the second row shows that the second-harmonic signal is practically zero in reflection and transmission if the incoming fields have different helicities. These results agree entirely with the selection rules shown in Fig. 2 for $n = 3$.

Incident	Transm. (arb. units)		Refl. (arb. units)	
	TE	TM	TE	TM
TE-TE	9.11e-10	0.498	9.11e-10	0.498
TM-TM	1.42e-09	1	1.42e-09	1
TE-TM	0.383	2.44e-09	0.383	2.44e-09

TABLE II. Simulated SHG signal for the rhomboid structure. The fundamental wavelength is 800 nm. The incoming and outgoing polarizations are in the TE/TM basis, and the numbers are normalized to 6.1×10^{-34} .

Incident	Transm. (arb. units)		Refl. (arb. units)	
	+	-	+	-
++	0.160	0.254	0.254	0.160
+-	0.359	0.359	0.359	0.359

TABLE III. Simulated SHG signal for the rhomboid structure. The fundamental wavelength is 800 nm. The incoming and outgoing polarizations are in the helicity basis, and the numbers are normalized to 6.1×10^{-34} .

Incident	Transm. (arb. units)		Refl. (arb. units)	
	+	-	+	-
++	4.29e-06	0.139	0.139	4.29e-06
+-	3.67e-05	3.64e-05	3.64e-05	3.67e-05

TABLE IV. Simulated SHG signal for the C₃-symmetric structure. The fundamental wavelength is 800 nm. The incoming and outgoing polarizations are in the helicity basis, and the numbers are normalized to 6.1×10^{-34} .

VI. THE T-MATRIX IN \mathbb{M}_2

The derivation of the selection rules in Sec. IV C does not require explicit knowledge of the scattering operator S_2 . One only needs to know the symmetries of the object and apply the corresponding operators to the incoming and outgoing states. While we have focused on non-linear processes, the selection rules can be readily obtained for bipartite scattering processes where the outgoing fields do not contain frequencies that are not already contained in the incoming fields. In this section, we investigate how to compute S_2 for both this case and for the non-linear case. We do so by considering the T-matrix in \mathbb{M}_2 .

Let us use the structure of \mathbb{M}_2 to arrive at T_2 , the T-matrix for bipartite states. First, we consider the relation between S and T for states in \mathbb{M} :

$$S = \mathbb{1} + T. \quad (55)$$

The difference with the typical relation $S = \mathbb{1} + 2T$ is due to the conventions in [27], which are more appropriate for the polychromatic case.

While the scattering operator S describes the connection between the incoming and outgoing fields, the T-matrix describes the connection between the incident and scattered fields. The incident field has both incoming and outgoing components, and the scattered field is a part of the total outgoing field. The outgoing field is the scattered field plus the outgoing part of the incident field,

and the incoming field is the incoming part of the incident field.

For the scattering operator in the bipartite space, we may define S_2 in a separable way

$$S_2 = S \otimes S \quad (56)$$

which, using Eq. (55), results in

$$\begin{aligned} S_2 &= \mathbb{1} \otimes \mathbb{1} + \mathbb{1} \otimes T + T \otimes \mathbb{1} + T \otimes T \\ \implies T_2 &= \mathbb{1} \otimes T + T \otimes \mathbb{1} + T \otimes T. \end{aligned} \quad (57)$$

Note that Eq. (57) seems to disagree with existing literature, see, e.g., [51], where only the last term $T \otimes T$ is used as T_2 . We now give arguments in favor of the definition in Eq. (56). Let us assume that the scattering is lossless

in \mathbb{M} , implying

$$S^\dagger S = \mathbb{1} \Leftrightarrow T + T^\dagger + T^\dagger T = 0. \quad (58)$$

If the scattering is lossless in \mathbb{M} , then the bipartite scattering should also be lossless. In that case, only the definition in Eq. (56) ensures that S_2 is unitary, meaning $S_2^\dagger S_2 = (S^\dagger \otimes S^\dagger)(S \otimes S) = \mathbb{1} \otimes \mathbb{1}$. Another feature of Eq. (56) is that each of the terms in T_2 in Eq. (57) has an intuitive physical meaning: The first two terms describe the interaction of only one of the two parts of the incident bipartite states. In contrast, the third term describes the interaction of both parts.

Let us now study the action of T_2 on a general bipartite plane wave state. We find

$$\begin{aligned} T_2 |\mathbf{k} \lambda, \bar{\mathbf{k}} \bar{\lambda}\rangle_2 &= (\mathbb{1} \otimes T + T \otimes \mathbb{1} + T \otimes T) \frac{1}{\sqrt{2}} (|\mathbf{k} \lambda\rangle \otimes |\bar{\mathbf{k}} \bar{\lambda}\rangle + |\bar{\mathbf{k}} \bar{\lambda}\rangle \otimes |\mathbf{k} \lambda\rangle) \\ &= |T\{\mathbf{k} \lambda\}, \bar{\mathbf{k}} \bar{\lambda}\rangle_2 + |\mathbf{k} \lambda, T\{\bar{\mathbf{k}} \bar{\lambda}\}\rangle_2 + |T\{\mathbf{k} \lambda\}, T\{\bar{\mathbf{k}} \bar{\lambda}\}\rangle_2, \end{aligned} \quad (59)$$

using the notation

$$\begin{aligned} |T\{\mathbf{k} \lambda\}, \bar{\mathbf{k}} \bar{\lambda}\rangle_2 &\equiv \frac{1}{\sqrt{2}} (T|\mathbf{k} \lambda\rangle \otimes |\bar{\mathbf{k}} \bar{\lambda}\rangle + |\bar{\mathbf{k}} \bar{\lambda}\rangle \otimes T|\mathbf{k} \lambda\rangle), \\ |T\{\mathbf{k} \lambda\}, T\{\bar{\mathbf{k}} \bar{\lambda}\}\rangle_2 &\equiv \frac{1}{\sqrt{2}} (T|\mathbf{k} \lambda\rangle \otimes T|\bar{\mathbf{k}} \bar{\lambda}\rangle \\ &\quad + T|\bar{\mathbf{k}} \bar{\lambda}\rangle \otimes T|\mathbf{k} \lambda\rangle). \end{aligned} \quad (60)$$

Equation (59) states that the scattered bipartite plane wave consists of a superposition of three bipartite states,

where in the first two states, either one part of the bipartite state interacts with the object, and in the third state both parts interact with the object. Let us write it more explicitly by expressing the T-matrix in the plane wave basis

$$\begin{aligned} T &= \sum_{\sigma\bar{\sigma}} \int \frac{d^3\mathbf{q}}{|\mathbf{q}|} \frac{d^3\bar{\mathbf{q}}}{|\bar{\mathbf{q}}|} T_{\sigma\bar{\sigma}}(\mathbf{q}, \bar{\mathbf{q}}) |\mathbf{q} \sigma\rangle \langle \bar{\mathbf{q}} \bar{\sigma}|, \\ T_{\sigma\bar{\sigma}}(\mathbf{q}, \bar{\mathbf{q}}) &= \langle \mathbf{q} \sigma | T | \bar{\mathbf{q}} \bar{\sigma} \rangle \end{aligned} \quad (61)$$

with which we can recast the last term in Eq. (59), yielding

$$|T\{\mathbf{k} \lambda\}, T\{\bar{\mathbf{k}} \bar{\lambda}\}\rangle_2 = \frac{1}{\sqrt{2}} \sum_{\sigma} \int \frac{d^3\mathbf{q}}{|\mathbf{q}|} T_{\sigma\lambda}(\mathbf{q}, \mathbf{k}) |\mathbf{q} \sigma\rangle \otimes \sum_{\bar{\sigma}} \int \frac{d^3\bar{\mathbf{q}}}{|\bar{\mathbf{q}}|} T_{\bar{\sigma}\bar{\lambda}}(\bar{\mathbf{q}}, \bar{\mathbf{k}}) |\bar{\mathbf{q}} \bar{\sigma}\rangle \quad (62)$$

$$+ \frac{1}{\sqrt{2}} \sum_{\bar{\sigma}} \int \frac{d^3\bar{\mathbf{q}}}{|\bar{\mathbf{q}}|} T_{\bar{\sigma}\bar{\lambda}}(\bar{\mathbf{q}}, \bar{\mathbf{k}}) |\bar{\mathbf{q}} \bar{\sigma}\rangle \otimes \sum_{\sigma} \int \frac{d^3\mathbf{q}}{|\mathbf{q}|} T_{\sigma\lambda}(\mathbf{q}, \mathbf{k}) |\mathbf{q} \sigma\rangle \quad (63)$$

$$= \frac{1}{\sqrt{2}} \sum_{\sigma\bar{\sigma}} \int \frac{d^3\mathbf{q}}{|\mathbf{q}|} \frac{d^3\bar{\mathbf{q}}}{|\bar{\mathbf{q}}|} T_{\sigma\lambda}(\mathbf{q}, \mathbf{k}) T_{\bar{\sigma}\bar{\lambda}}(\bar{\mathbf{q}}, \bar{\mathbf{k}}) (|\mathbf{q} \sigma\rangle |\bar{\mathbf{q}} \bar{\sigma}\rangle + |\bar{\mathbf{q}} \bar{\sigma}\rangle |\mathbf{q} \sigma\rangle) \quad (64)$$

$$= \sum_{\sigma\bar{\sigma}} \int \frac{d^3\mathbf{q}}{|\mathbf{q}|} \frac{d^3\bar{\mathbf{q}}}{|\bar{\mathbf{q}}|} T_{\sigma\lambda}(\mathbf{q}, \mathbf{k}) T_{\bar{\sigma}\bar{\lambda}}(\bar{\mathbf{q}}, \bar{\mathbf{k}}) |\mathbf{q} \sigma, \bar{\mathbf{q}} \bar{\sigma}\rangle_2. \quad (65)$$

One can now use that $\langle \mathbf{k} \lambda | \bar{\mathbf{k}} \bar{\lambda} \rangle = |\mathbf{k}| \delta_{\lambda\bar{\lambda}} \delta(\mathbf{k} - \bar{\mathbf{k}})$ to readily compute the scattering amplitude:

$$\begin{aligned} {}_2\langle \mathbf{p} \eta, \bar{\mathbf{p}} \bar{\eta} | T\{\mathbf{k} \lambda\}, T\{\bar{\mathbf{k}} \bar{\lambda}\} \rangle_2 \\ = T_{\eta\lambda}(\bar{\mathbf{p}}, \mathbf{k}) T_{\bar{\eta}\bar{\lambda}}(\mathbf{p}, \bar{\mathbf{k}}) + T_{\eta\lambda}(\mathbf{p}, \mathbf{k}) T_{\bar{\eta}\bar{\lambda}}(\bar{\mathbf{p}}, \bar{\mathbf{k}}). \end{aligned} \quad (66)$$

The assumption in the separable expression of S_2 in

Eq. (56) is that the response of the object to one part of the bipartite state does not depend on the other part. This applies in particular to biphoton states interacting with nanoparticles [8, 9, 51], where the $T \otimes T$ term has been the focus of attention. In the separable case, one only needs the knowledge of T , the T-matrix in \mathbb{M} , as is

evident from Eq. (66).

We are further interested in incorporating non-linear processes such as SFG into this formalism. The intensity of the incoming states causes the response of the material to depend on the incoming fields. To proceed, we write the following amplitude for an SFG process, where the outgoing state is given by $|\mathbf{k}_2 \lambda_2, 0\rangle_2$, with $|\mathbf{k}_2| = |\mathbf{k}| + |\bar{\mathbf{k}}|$

$$\begin{aligned} & {}_2\langle \mathbf{k}_2 \lambda_2, 0 | T \{ |\mathbf{k} \lambda\rangle, T \{ |\bar{\mathbf{k}} \bar{\lambda}\rangle \} \rangle_2 \\ &= \langle \mathbf{k}_2 \lambda_2 | T | \mathbf{k} \lambda \rangle \langle 0 | T | \bar{\mathbf{k}} \bar{\lambda} \rangle + \langle \mathbf{k}_2 \lambda_2 | T | \bar{\mathbf{k}} \bar{\lambda} \rangle \langle 0 | T | \mathbf{k} \lambda \rangle. \end{aligned} \quad (67)$$

This expression becomes interesting with the following interpretation. For SFG to happen, two fields need to be incident on some object described by T . As a first step, one of the two incident fields perturbs the object. Such a perturbation, which is described by $\langle 0 | T | \bar{\mathbf{k}} \bar{\lambda} \rangle$ or $\langle 0 | T | \mathbf{k} \lambda \rangle$, excites current sources in the object with frequency $c|\bar{\mathbf{k}}|$ or $c|\mathbf{k}|$, respectively. Therefore, the interaction of the second field with the perturbed system yields an outgoing field with the total energy of the two incident fields. The interaction of the second field is described by the T -matrix of the object after perturbation by a first field $\langle \mathbf{k}_2 \lambda_2 | T | \mathbf{k} \lambda \rangle$, or $\langle \mathbf{k}_2 \lambda_2 | T | \bar{\mathbf{k}} \bar{\lambda} \rangle$. An element such as $\langle 0 | T | \bar{\mathbf{k}} \bar{\lambda} \rangle$ can be interpreted as a transition to the vacuum, that is, as absorption by the object. Then, Eq. (67) implies that there cannot be SFG unless at least one of the two parts of the bipartite state has a non-zero probability of being absorbed by the object. However, it should be noted that the calculation of $\langle 0 | T | \bar{\mathbf{k}} \bar{\lambda} \rangle$ cannot be the standard one: If one uses the straightforward expansion of T into plane waves in Eq. (61), the result would be a linear combination of terms containing a vanishing $\langle 0 | \mathbf{q} \bar{\lambda} \rangle$ element. A different interpretation of $\langle 0 | T | \bar{\mathbf{k}} \bar{\lambda} \rangle$ should be possible since, contrary to propagation in free space, the interaction with matter can result in the absorption of the photon. Devising computational strategies for obtaining the terms $\langle \mathbf{k}_2 \lambda_2 | T | \mathbf{k} \lambda \rangle \langle 0 | T | \bar{\mathbf{k}} \bar{\lambda} \rangle$ is a subject of further research. We envision the total S_2 to be a combination of this part describing non-linear processes, and the operator in Eq. (57) where the T-matrices have the typical meaning in \mathbb{M} .

It is reassuring to find that one can readily verify the physical intuition that the other pieces of T_2 , namely $\mathbb{1} \otimes T + T \otimes \mathbb{1}$ cannot contribute to SFG because only one part of the state interacts with the object. Each term of the amplitude

$${}_2\langle \mathbf{k}_2 \lambda_2, 0 | \mathbb{1} \otimes T + T \otimes \mathbb{1} | \mathbf{k} \lambda, \bar{\mathbf{k}} \bar{\lambda} \rangle_2 \quad (68)$$

contains the scalar product of the vacuum state with a plane wave state, which vanishes.

The fact that one of the parts of the state affects the response of the material to the other suggests that non-linear responses can be incorporated into the scattering formalism through a *non-separable* S_2 operator. That is, when

$$S_{2,\lambda\bar{\lambda}\sigma\bar{\sigma}}(\mathbf{k}, \bar{\mathbf{k}}, \mathbf{q}, \bar{\mathbf{q}}) \neq S_{\lambda\bar{\lambda}}(\mathbf{k}, \bar{\mathbf{k}}) S_{\sigma\bar{\sigma}}(\mathbf{q}, \bar{\mathbf{q}}), \quad (69)$$

which is in contrast to the definition of S_2 in Eq. (56).

The above interpretations of Eq. (67) connect with descriptions of SFG that use second-order perturbation theory [12, Chap. 3], where the second-order term is obtained as a perturbation of an already perturbed system, where the first and second perturbations are due to the first and second parts of a bipartite state, respectively. Procedures such as second-order perturbation result in effective computational strategies for non-linear optical processes in microscopic systems such as molecules. Then, the non-linear response of some macroscopic objects built out of large ensembles of microscopic systems can be obtained, as in [32], where the non-linear molecular hyperpolarizabilities of the unit cells of molecular crystals are mapped into corresponding Hyper-T-matrices. The calculation of the non-linear response of crystals of macroscopic sizes becomes feasible.

The above discussion prompts the question of whether it is possible to obtain a description of the non-linear response of general macroscopic objects by considering the interaction of a field with a macroscopic object that has already been perturbed by another field. The time-dependent perturbation induced by the first field suggests that this question could be addressed with the tools that are being developed to treat light-matter interaction in time-varying systems [52]. Note that, if successful, such an approach would include the SH signal generated on the interfaces between different materials. This latter effect happens in addition to the SH signal produced in the bulk of a given material, which, to a first approximation, is only possible if the unit cell of the material is not centrosymmetric. While the surface SHG of molecular films has been recently simulated *ab initio* [53], the theoretical approach to surface SHG for macroscopic objects, such as a silicon disk, for instance, is to add a phenomenological tensor on the surface to allow for the SHG [54].

VII. CONCLUSION AND OUTLOOK

In this article, we set the basis for the algebraic treatment of the interaction of bipartite states of light with nanostructures. Such a basis allows one to readily derive symmetry-induced selection rules and facilitates the study of entanglement evolution upon light-matter interaction. We have theoretically obtained and numerically verified selection rules for sum-frequency generation in objects featuring rotational and/or mirror symmetries. The treatment of non-linear processes requires the inclusion of a vacuum state, with which single photon states can be written as bipartite states containing the vacuum. We derive the T-matrix for bipartite states, which has a straightforward dependence on the T-matrix for single photons when non-linear processes are not considered.

The results in this article motivate further research, for example regarding the integration of non-linear processes in the formalism, as discussed in Sec. VI. In this article, we have used the plane wave basis, however, obtaining the expression of the bipartite wavefunction and the scalar product in \mathbb{M}_2 in the multipolar basis is interesting for computations as well, since T-matrices are often computed in such basis. On the theoretical side, the for-

malism can be further developed by using the invariant properties of the scalar product to formalize projective measurements in \mathbb{M}_2 . Additionally, the transformation properties of biphoton states under Lorentz boosts can be obtained, which would be useful for satellite quantum communications.

We foresee that the algebraic formalism will become a useful tool for studying and engineering of the interaction of bipartite states of light with nanostructures and arrangements thereof.

ACKNOWLEDGMENTS

L.F. wishes to acknowledge the support from the Jane and Aatos Erkkö Foundation under the “DoinQTech” project. M.K. and C.R. acknowledge support by the Deutsche Forschungsgemeinschaft (DFG, German Re-

search Foundation) under Germany’s Excellence Strategy via the Excellence Cluster 3D Matter Made to Order (EXC-2082/1-390761711) and from the Carl Zeiss Foundation via the CZF-Focus@HEiKA Program. M.K., C.H., and C.R. acknowledge funding by the Volkswagen Foundation. I.F.C. and C.R. acknowledge support by the Helmholtz Association via the Helmholtz program “Materials Systems Engineering” (MSE). B.Z. and C.R. acknowledge support by the KIT through the “Virtual Materials Design” (VIRTMAT) project. M.K. and C.R. acknowledge support by the state of Baden–Württemberg through bwHPC and the German Research Foundation (DFG) through grant no. INST 40/575-1 FUGG (JUSTUS 2 cluster) and the HoreKa supercomputer funded by the Ministry of Science, Research and the Arts Baden–Württemberg and by the Federal Ministry of Education and Research.

-
- [1] L. Huang, L. Xu, M. Woolley, and A. E. Miroshnichenko, Trends in quantum nanophotonics, *Advanced Quantum Technologies* **3**, 1900126 (2020).
- [2] A. S. Solntsev, G. S. Agarwal, and Y. S. Kivshar, Metasurfaces for quantum photonics, *Nature Photonics* **15**, 327 (2021).
- [3] C. Ioannou, R. Nair, I. Fernandez-Corbaton, M. Gu, C. Rockstuhl, and C. Lee, Optimal circular dichroism sensing with quantum light: Multiparameter estimation approach, *Phys. Rev. A* **104**, 052615 (2021).
- [4] C. Oh, L. Jiang, and C. Lee, Distributed quantum phase sensing for arbitrary positive and negative weights, *Phys. Rev. Res.* **4**, 023164 (2022).
- [5] K. Wang, J. G. Titchener, S. S. Kruk, L. Xu, H.-P. Chung, M. Parry, I. I. Kravchenko, Y.-H. Chen, A. S. Solntsev, Y. S. Kivshar, D. N. Neshev, and A. A. Sukhorukov, Quantum metasurface for multiphoton interference and state reconstruction, *Science* **361**, 1104 (2018).
- [6] A. Vega, T. Pertsch, F. Setzpfandt, and A. A. Sukhorukov, Metasurface-assisted quantum ghost discrimination of polarization objects, *Phys. Rev. Appl.* **16**, 064032 (2021).
- [7] J. Ma, J. Zhang, J. Horder, A. A. Sukhorukov, M. Toth, D. N. Neshev, and I. Aharonovich, Engineering quantum light sources with flat optics, *Advanced Materials* , 2313589 (2024).
- [8] A. Büse, M. L. Juan, N. Tischler, V. D’Ambrosio, F. Sciarrino, L. Marrucci, and G. Molina-Terriza, Symmetry protection of photonic entanglement in the interaction with a single nanoaperture, *Phys. Rev. Lett.* **121**, 173901 (2018).
- [9] J. Lasa-Alonso, M. Molezuelas-Ferreras, J. J. M. Varga, A. García-Etxarri, G. Giedke, and G. Molina-Terriza, Symmetry-protection of multiphoton states of light, *New Journal of Physics* **22**, 123010 (2020).
- [10] N. Tischler, *Towards quantum metrology for nanoscatterers*, Ph.D. thesis, Macquarie University (2022).
- [11] P. N. Butcher and D. Cotter, *The elements of nonlinear optics* (Cambridge University Press, 1990).
- [12] R. W. Boyd, *Nonlinear Optics*, fourth edition ed. (Academic Press, 2020).
- [13] K. Frizyuk, I. Volkovskaya, D. Smirnova, A. Poddubny, and M. Petrov, Second-harmonic generation in Mie-resonant dielectric nanoparticles made of noncentrosymmetric materials, *Phys. Rev. B* **99**, 075425 (2019).
- [14] K. Frizyuk, Second-harmonic generation in dielectric nanoparticles with different symmetries, *J. Opt. Soc. Am. B* **36**, F32 (2019).
- [15] R. Sarma, J. Xu, D. de Ceglia, L. Carletti, S. Campione, J. Klem, M. B. Sinclair, M. A. Belkin, and I. Brener, An all-dielectric polaritonic metasurface with a giant nonlinear optical response, *Nano Letters* **22**, 896 (2022).
- [16] A. Fedotova, M. Younesi, M. Weissflog, D. Arslan, T. Pertsch, I. Staude, and F. Setzpfandt, Spatially engineered nonlinearity in resonant metasurfaces, *Photon. Res.* **11**, 252 (2023).
- [17] T. Santiago-Cruz, A. Fedotova, V. Sultanov, M. A. Weissflog, D. Arslan, M. Younesi, T. Pertsch, I. Staude, F. Setzpfandt, and M. Chekhova, Photon Pairs from Resonant Metasurfaces, *Nano Letters* **21**, 4423 (2021), publisher: American Chemical Society.
- [18] M. Sharma, M. Tal, C. McDonnell, and T. Ellenbogen, Electrically and all-optically switchable nonlocal nonlinear metasurfaces, *Science Advances* **9**, eadh2353 (2023).
- [19] L. Bonacina, P.-F. Brevet, M. Finazzi, and M. Celebrano, Harmonic generation at the nanoscale, *Journal of Applied Physics* **127**, 230901 (2020).
- [20] A. Verneuil, A. D. Francescantonio, A. Zilli, J. Proust, J. Béal, D. Petti, M. Finazzi, M. Celebrano, and A.-L. Baudrion, Far-field mapping and efficient beaming of second harmonic by a plasmonic metagrating, *Nanophotonics* 10.1515/nanoph-2023-0842 (2024), publisher: De Gruyter.
- [21] P. C. Waterman, Matrix formulation of electromagnetic scattering, *Proc. IEEE* **53**, 805 (1965).
- [22] G. Gouesbet, T-matrix methods for electromagnetic structured beams: A commented reference database for the period 2014–2018, *Journal of Quantitative Spectroscopy and Radiative Transfer* **230**, 247 (2019).
- [23] M. I. Mishchenko, Comprehensive thematic t-matrix reference database: a 2017-2019 update, *Journal of Quantitative Spectroscopy and Radiative Transfer* **242**, 106692 (2020).
- [24] I. Fernandez-Corbaton, D. Beutel, C. Rockstuhl,

- A. Pausch, and W. Klopper, Computation of electromagnetic properties of molecular ensembles, *ChemPhysChem* **21**, 878 (2020).
- [25] D. Beutel, I. Fernandez-Corbaton, and C. Rockstuhl, treams – a t-matrix-based scattering code for nanophotonics, *Computer Physics Communications* **297**, 109076 (2024).
- [26] Scattport website, <https://scattport.org/index.php/light-scattering-software/t-matrix-codes>.
- [27] M. Vavilin and I. Fernandez-Corbaton, The polychromatic T-matrix, *Journal of Quantitative Spectroscopy and Radiative Transfer* **314**, 108853 (2024).
- [28] L. Gross, Norm invariance of Mass-Zero equations under the conformal group, *J. Math. Phys.* **5**, 687 (1964).
- [29] I. Fernandez-Corbaton and M. Vavilin, A scalar product for computing fundamental quantities in matter, *Symmetry* **15**, 10.3390/sym15101839 (2023).
- [30] Y. Shih, Entangled biphoton source - property and preparation, *Reports on Progress in Physics* **66**, 1009 (2003).
- [31] S. Carrasco, J. P. Torres, L. Torner, A. Sergienko, B. E. A. Saleh, and M. C. Teich, Spatial-to-spectral mapping in spontaneous parametric down-conversion, *Phys. Rev. A* **70**, 043817 (2004).
- [32] B. Zerulla, D. Beutel, C. Holzer, I. Fernandez-Corbaton, C. Rockstuhl, and M. Krstić, A multi-scale approach to simulate the nonlinear optical response of molecular nanomaterials, *Advanced Materials* **36**, 2311405 (2024).
- [33] M. Vavilin, J. D. Mazo-Vásquez, and I. Fernandez-Corbaton, Computing the interaction of light pulses with objects moving at relativistic speeds (2024), arXiv:2404.05117 [physics.optics].
- [34] Z. Bern, T. Dennen, Y.-t. Huang, and M. Kiermaier, Gravity as the square of gauge theory, *Phys. Rev. D* **82**, 065003 (2010).
- [35] Z. Bern, J. J. M. Carrasco, and H. Johansson, Perturbative quantum gravity as a double copy of gauge theory, *Phys. Rev. Lett.* **105**, 061602 (2010).
- [36] I. Fernandez-Corbaton, M. Cirio, A. Büse, L. Lamata, E. Solano, and G. Molina-Terriza, Quantum emulation of gravitational waves, *Sci. Rep.* **5**, 11538 (2015).
- [37] C. Cheung and G. N. Remmen, Entanglement and the double copy, *Journal of High Energy Physics* **2020**, 100 (2020).
- [38] C. D. White, Double copy—from optics to quantum gravity: tutorial, *J. Opt. Soc. Am. B* **38**, 3319 (2021).
- [39] I. Fernandez-Corbaton, *Helicity and duality symmetry in light matter interactions: Theory and applications*, Ph.D. thesis, Macquarie University (2015).
- [40] Fernandez-Corbaton, Ivan, The optical helicity in a more algebraic approach to electromagnetism, *Photoniques* **113**, 54 (2022).
- [41] Y. B. Zel'dovich, The number of quanta as an invariant of classical electromagnetic field, *Doklady Akademii Nauk SSSR (USSR) English translation currently published in a number of subject-oriented journals* **163** (1965).
- [42] I. Bialynicki-Birula, V Photon Wave Function, in *Progress in Optics*, Vol. 36, edited by E. Wolf (Elsevier, 1996) pp. 245–294.
- [43] I. Fernandez-Corbaton, Forward and backward helicity scattering coefficients for systems with discrete rotational symmetry, *Optics Express* **21**, 29885 (2013).
- [44] A. Altland and B. Simons, *Condensed Matter Field Theory* (Cambridge University Press, 2006).
- [45] H. Bateman, The transformation of the electrodynamic equations, *Proceedings of the London Mathematical Society* **s2-8**, 223 (1910).
- [46] W.-K. Tung, *Group Theory in Physics* (World Scientific, 1985).
- [47] R. F. Streater and A. S. Wightman, *PCT, Spin and Statistics, and All That* (Princeton University Press, 1989).
- [48] C. L. Tang and H. Rabin, Selection Rules for Circularly Polarized Waves in Nonlinear Optics, *Physical Review B* **3**, 4025 (1971).
- [49] S. Bhagavantam and P. Chandrasekhar, Harmonic generation and selection rules in nonlinear optics, *Proceedings of the Indian Academy of Sciences - Section A* **76**, 13 (1972).
- [50] Y. Zhang, Y. Wang, Y. Dai, X. Bai, X. Hu, L. Du, H. Hu, X. Yang, D. Li, Q. Dai, T. Hasan, and Z. Sun, Chirality logic gates, *Science Advances* **8**, eabq8246 (2022).
- [51] J. C. Schotland, A. Cazé, and T. B. Norris, Scattering of entangled two-photon states, *Optics Letters* **41**, 444 (2016).
- [52] G. Ptitsyn, A. Lamprianidis, T. Karamanos, V. Asadchy, R. Alaee, M. Müller, M. Albooyeh, M. S. Mirmoosa, S. Fan, S. Tretyakov, and C. Rockstuhl, Floquet-mie theory for time-varying dispersive spheres, *Laser & Photonics Reviews* **17**, 2100683 (2023).
- [53] B. Zerulla, A. L. Díaz, C. Holzer, C. Rockstuhl, I. Fernandez-Corbaton, and M. Krstić, Surface second harmonic generation in centrosymmetric molecular crystalline materials: How thick is the surface?, accepted for publication, arXiv:2310.20297 [physics.optics].
- [54] J. I. Dadap, J. Shan, and T. F. Heinz, Theory of optical second-harmonic generation from a sphere of centrosymmetric material: small-particle limit, *J. Opt. Soc. Am. B* **21**, 1328 (2004).
- [55] TURBOMOLE 7.8 (2023).
- [56] C. Adamo and V. Barone, Toward reliable density functional methods without adjustable parameters: The PBE0 model, *J. Chem. Phys.* **110**, 6158 (1999).
- [57] M. Ernzerhof and G. E. Scuseria, Assessment of the Perdew–Burke–Ernzerhof exchange–correlation functional, *J. Chem. Phys.* **110**, 5029 (1999).
- [58] F. Weigend and R. Ahlrichs, Balanced basis sets of split valence, triple zeta valence and quadruple zeta valence quality for H to Rn: Design and assessment of accuracy, *Phys. Chem. Chem. Phys.* **7**, 3297 (2005).
- [59] F. Weigend, Accurate Coulomb-fitting basis sets for H to Rn, *Phys. Chem. Chem. Phys.* **8**, 1057 (2006).
- [60] K. Eichkorn, O. Treutler, H. Öhm, M. Häser, and R. Ahlrichs, Auxiliary basis sets to approximate Coulomb potentials (*Chem. Phys. Letters* 240 (1995) 283–290), *Chem. Phys. Lett.* **242**, 652 (1995).
- [61] K. Eichkorn, F. Weigend, O. Treutler, and R. Ahlrichs, Auxiliary basis sets for main row atoms and transition metals and their use to approximate Coulomb potentials, *Theor. Chem. Acta* **97**, 119 (1997).
- [62] M. Sierka, A. Hogekamp, and R. Ahlrichs, Fast evaluation of the Coulomb potential for electron densities using multipole accelerated resolution of identity approximation, *J. Chem. Phys.* **118**, 9136 (2003).
- [63] C. Holzer, An improved seminumerical Coulomb and exchange algorithm for properties and excited states in modern density functional theory, *The Journal of Chemical Physics* **153**, 184115 (2020).

VIII. SUPPLEMENTARY INFORMATION

A. Details of the Density Functional Theory (DFT) calculations

A single layer of MoS₂ crystal was extracted from the crystallography file given below. The two distinctive finite-size models were cut out in the shape of an approximate hexagon and rhomboid. Single point energy calculations of those models were performed using the development version of TURBOMOLE 7.8[55], followed by calculation of linear polarizability tensors at fundamental and second-harmonic frequency and first hyperpolarizability tensors. A PBE0[56, 57] hybrid exchange-correlation (XC) density functional has been used in combination with def2-TZVP basis set[58, 59] for all atoms. Molybdenum atoms had Stuttgart relativistic effective core potential to reduce the number of explicitly treated electrons by replacing the core electrons by a potential. A numerical grid size was set to "3". The damping was 0.05 eV for the Lorentzian line-shape profile at half-width at half-maximum (HWHM). To speed up the calculations, the multipole-accelerated resolution-of-the-identity (MARI-J)[60–62] and semi-numerical approach for the exchange (senex, esenex)[63] have been employed.

MoS₂ cif file used to extract finite-size molecular models:

```
# generated using pymatgen
data_MoS2
_symmetry_space_group_name_H-M 'P 1'
_cell_length_a 3.19031570
_cell_length_b 3.19031570
_cell_length_c 14.87900400
_cell_angle_alpha 90.00000000
_cell_angle_beta 90.00000000
_cell_angle_gamma 120.00000000
_symmetry_Int_Tables_number 1
_chemical_formula_structural MoS2
_chemical_formula_sum 'Mo2 S4'
_cell_volume 131.15106251
_cell_formula_units_Z 2
loop_
  _symmetry_equiv_pos_site_id
  _symmetry_equiv_pos_as_xyz
  1 'x, y, z'
loop_
  _atom_type_symbol
  _atom_type_oxidation_number
  Mo4+ 4.0
  S2- -2.0
loop_
  _atom_site_type_symbol
  _atom_site_label
  _atom_site_symmetry_multiplicity
  _atom_site_fract_x
  _atom_site_fract_y
  _atom_site_fract_z
```

```
_atom_site_occupancy
Mo4+ Mo0 1 0.33333333 0.66666667 0.25000000 1
Mo4+ Mo1 1 0.66666667 0.33333333 0.75000000 1
S2- S2 1 0.66666667 0.33333333 0.35517400 1
S2- S3 1 0.33333333 0.66666667 0.85517400 1
S2- S4 1 0.66666667 0.33333333 0.14482600 1
S2- S5 1 0.33333333 0.66666667 0.64482600 1
```

Cartesian coordinates of both molecular models:

Approximate hexagon:

55

```
Mo -0.00000 6.38063 -0.00000
Mo -0.00000 4.78547 2.76291
Mo -0.00000 3.19032 5.52579
Mo -0.00000 4.78547 -2.76289
Mo -0.00000 3.19032 -0.00000
Mo -0.00000 1.59516 2.76291
Mo -0.00000 -0.00000 5.52579
Mo -0.00000 3.19032 -5.52579
Mo -0.00000 1.59516 -2.76289
Mo -0.00000 -0.00000 -0.00000
Mo -0.00000 -1.59516 2.76291
Mo -0.00000 -3.19032 5.52579
Mo -0.00000 -0.00000 -5.52579
Mo -0.00000 -1.59516 -2.76289
Mo -0.00000 -3.19032 -0.00000
Mo -0.00000 -4.78547 2.76291
Mo -0.00000 -3.19032 -5.52579
Mo -0.00000 -4.78547 -2.76289
Mo -0.00000 -6.38063 -0.00000
S -1.56488 6.38063 1.84193
S -1.56488 4.78547 4.60483
S -1.56488 4.78547 -0.92096
S -1.56488 3.19032 1.84193
S -1.56488 1.59516 4.60483
S -1.56488 3.19032 -3.68386
S -1.56488 1.59516 -0.92096
S -1.56488 -0.00000 1.84193
S -1.56488 -1.59516 4.60483
S -1.56488 1.59516 -6.44675
S -1.56488 -0.00000 -3.68386
S -1.56488 -1.59516 -0.92096
S -1.56488 -3.19032 1.84193
S -1.56488 -4.78547 4.60483
S -1.56488 -1.59516 -6.44675
S -1.56488 -3.19032 -3.68386
S -1.56488 -4.78547 -0.92096
S -1.56488 -6.38063 1.84193
S 1.56488 6.38063 1.84193
S 1.56488 4.78547 4.60483
S 1.56488 4.78547 -0.92096
S 1.56488 3.19032 1.84193
S 1.56488 1.59516 4.60483
S 1.56488 3.19032 -3.68386
S 1.56488 1.59516 -0.92096
S 1.56488 -0.00000 1.84193
S 1.56488 -1.59516 4.60483
S 1.56488 1.59516 -6.44675
S 1.56488 -0.00000 -3.68386
S 1.56488 -1.59516 -0.92096
```

```
S 1.56488 -3.19032 1.84193
S 1.56488 -4.78547 4.60483
S 1.56488 -1.59516 -6.44675
S 1.56488 -3.19032 -3.68386
S 1.56488 -4.78547 -0.92096
S 1.56488 -6.38063 1.84193
```

Rhomboid:
27

```
Mo -0.00000 3.19031 -0.73794
Mo -0.00000 1.59515 2.02495
Mo -0.00000 0.00000 4.78785
Mo -0.00000 1.59515 -3.50084
Mo -0.00000 0.00000 -0.73794
Mo -0.00000 -1.59516 2.02495
Mo -0.00000 0.00000 -6.26373
Mo -0.00000 -1.59516 -3.50084
Mo -0.00000 -3.19032 -0.73794
S -1.56488 3.19031 1.10399
S -1.56488 1.59515 3.86688
S -1.56488 0.00000 6.62978
S -1.56488 1.59515 -1.65891
S -1.56488 0.00000 1.10399
S -1.56488 -1.59516 3.86688
S -1.56488 0.00000 -4.42180
S -1.56488 -1.59516 -1.65891
S -1.56488 -3.19032 1.10399
S 1.56488 3.19031 1.10399
S 1.56488 1.59515 3.86688
S 1.56488 0.00000 6.62978
S 1.56488 1.59515 -1.65891
S 1.56488 0.00000 1.10399
S 1.56488 -1.59516 3.86688
S 1.56488 0.00000 -4.42180
S 1.56488 -1.59516 -1.65891
S 1.56488 -3.19032 1.10399
```

An example of the "control" file for the calculation of the polarizabilities at 800 and 400 nm:

```
$title
$symmetry c1
$coord file=coord
$optimize
  internal off
  redundant off
  cartesian on
$atoms
  basis =def2-TZVP
  jbas =def2-TZVP
mo 1-19
  ecp =mo def2-ecp
$basis file=basis
$ecp file=basis
$scfmo file=mos
$scfiterlimit 1000
$scfdamp start=15.000 step=0.050 min=1.000
$scfdump
$scfdiis
  maxiter=20
```

```
$maxcor 1000 MiB per_core
$scforbitalshift automatic=.1
$energy file=energy
$grad file=gradient
$dft
  functional pbe0
  gridsize 3
$scfconv 7
$denconv 1.0d-7
$scftol 1.0d-16
$rundimensions
  natoms=55
$closed shells
  a 1-421 ( 2 )
$ricore 16000
$rjij
$jbas file=auxbasis
$marij
$scfiterlimit 2000
$scfinstab dynpol nm
  800
  400
$mgiao
$magnetic_response
$damped_response 0.05 eV
$rpacor 100000
$senex
  gridsize 1
$esenex
$last step define
$end
```

An example of the "control" file for the calculation of the first hyperpolarizabilities at 800 nm:

```
$title
$symmetry c1
$coord file=coord
$optimize
  internal off
  redundant off
  cartesian on
$atoms
  basis =def2-TZVP
  jbas =def2-TZVP
mo 1-19
  ecp =mo def2-ecp
$basis file=basis
$ecp file=basis
$scfmo file=mos
$scfiterlimit 1000
$scfdamp start=15.000 step=0.050 min=1.000
$scfdump
$scfdiis
  maxiter=20
$maxcor 1000 MiB per_core
$scforbitalshift automatic=.1
$energy file=energy
$grad file=gradient
$dft
  functional pbe0
```

```
    gridsize 3
$scfconv 7
$denconv 1.0d-7
$scftol 1.0d-16
$rundimensions
  natoms=55
$closed shells
  a 1-421 ( 2 )
$ricore 16000
$rij
$jbas file=auxbasis
$marij
```

```
$escfiterlimit 2000
$scfinstab hyperpol nm
  800
$mgiac
$damped_response 0.05 eV
$rpacor 100000
$senex
  gridsize 1
$esenex
$last step define
$end
```